

The variations of VOCs based on the policy change of Omicron in traffic-hub city Zhengzhou

Bowen Zhang^{1,3}, Dong Zhang^{2,3}, Zhe Dong^{2,3}, Xinshuai Song^{1,3}, Ruiqin Zhang^{1,3},
Xiao Li^{1,3,*}

¹School of Ecology and Environment, Zhengzhou University, Zhengzhou 450001,
China

²College of Chemistry, Zhengzhou University, Zhengzhou 450001, China

³Institute of Environmental Sciences, Zhengzhou University, Zhengzhou 450001,
China

Correspondence to: Xiao Li, E-mail address: lixiao9060@zzu.edu.cn

Abstract: Online volatile organic compounds (VOCs) were monitored before and after the Omicron policy change at an urban site in polluted Zhengzhou from December 1, 2022, to January 31, 2023. The characteristics and sources of VOCs were investigated. The daily mean concentrations of PM_{2.5} and total VOCs (TVOCs) ranged from 53.5 to 239.4 $\mu\text{g}/\text{m}^3$ and 15.6 to 57.1 ppbv, respectively, with mean values of $111.5 \pm 45.1 \mu\text{g}/\text{m}^3$ and 36.1 ± 21.0 ppbv, respectively, throughout the period. Two severe pollution events (designated as Case 1 and Case 2) were identified in accordance with the National Ambient Air Quality Standards (NAAQS) (China's National Ambient Air Quality Standards (NAAQS) from 2012). Case 1 (December 5 to December 10, PM_{2.5} daily mean = 142.5 $\mu\text{g}/\text{m}^3$) and Case 2 (January 1 to January 8, PM_{2.5} daily mean = 181.5 $\mu\text{g}/\text{m}^3$) occurred during the infection period (when the policy of "full nucleic acid screening measures" was in effect) and the recovery period (after the policy was cancelled), respectively. The PM_{2.5} and TVOCs values for Case 2 are, respectively, 1.3 and 1.8 times higher than those for Case 1. The precise influence of disparate meteorological circumstances on the two pollution incidents is not addressed in this study. The results of the positive matrix factor modeling demonstrated that the primary source of volatile organic compounds (VOCs) during the observation period was industrial emissions, which constituted 32% of the total VOCs, followed by vehicle emissions (27%) and combustion (21%). In Case 1, industrial emissions constituted the primary source of VOCs, accounting for 32% of the total VOCs. In contrast, in Case 2, the contribution of vehicular emission sources increased to 33% and became the primary source of VOCs. The secondary organic aerosol formation potential for Case 1 and Case 2 were found to be 37.6 $\mu\text{g}/\text{m}^3$ and 65.6 $\mu\text{g}/\text{m}^3$, respectively. In Case 1, the

34 largest contribution of SOAP from industrial sources accounted for the majority (63%,
35 23.8 $\mu\text{g}/\text{m}^3$), followed by vehicular sources (18%). After the end of the epidemic and
36 the resumption of productive activities in the society, the difference in the proportion
37 of SOA generated from various sources decreased. Most of the SOAP came from
38 solvent use and fuel evaporation sources, accounting for 32% (20.9 $\mu\text{g}/\text{m}^3$) and 26%
39 (16.8 $\mu\text{g}/\text{m}^3$), respectively. On days with minimal pollution, industrial sources and
40 solvent use remain the main contributors to SOA formation. Therefore, regulation of
41 emissions from industry, solvent-using industries and motor vehicles need to be
42 prioritized to control the $\text{PM}_{2.5}$ pollution problem.

43

44 **Keywords: Volatile organic compounds; Pollution episode; Source apportionment; Positive**
45 **Matrix Factorization model; Secondary organic aerosol formation potential;**

46 **1. Introduction**

47 Volatile organic compounds (VOCs) in the atmosphere have high reactivity and
48 can react with nitrogen oxides (NO_x) to form a series of secondary pollutants such as
49 ozone (O₃) and secondary organic aerosol (SOA), resulting in regional air pollution (Li
50 et al., 2019; Hui et al., 2020). The problem of O₃ pollution has been plaguing major
51 urban agglomerations in China (Zheng et al., 2010; Li et al., 2014; Wang et al., 2017).
52 SOA is an important component of fine particulate matter (PM_{2.5}) and contributes
53 significantly to haze pollution (Liu et al., 2019). PM_{2.5} remains the most significant air
54 pollutant in many Chinese cities for years (Shao et al., 2016; Wu et al., 2016). In
55 addition, VOCs, represented by the benzene homologues, can cause damage to kidneys,
56 liver, and nervous system of humans when they enter the body (Zhang et al., 2018).

57 Studies have shown that the most common VOC components in China are alkanes,
58 olefins, aromatic hydrocarbons, oxygenated VOCs (OVOCs), and halogenated
59 hydrocarbons, among which alkanes are the most abundant species (Liu et al., 2020;
60 Zhang et al., 2021a). VOCs in the atmosphere have a wide range of sources, and VOCs
61 in different regions are affected by multiple factors such as local geography, climate,
62 and human activities (Mu et al., 2023; Zou et al., 2023). The above reasons lead to
63 significant regional and seasonal differences in the characteristics of VOCs (Song et al.,
64 2021). For example, the annual average concentration of VOCs in the coastal
65 background area of the Pearl River Delta is 9.3 ppbv. The seasonal variation trend of
66 VOCs is high in autumn and winter and low in summer (Yun et al., 2021). In contrast,
67 the average VOC concentration in autumn and winter in Beijing was 22.6 ± 12.6 ppbv,
68 and the VOC concentration in the winter heating period was twice that in the autumn
69 non-heating period (Niu et al., 2022).

70 Moreover, the sources of VOC components in different regions are also related to
71 the local industrial structure and living habits. In rural areas of North China Plain in
72 winter, it is found that the SOA formation potential (SOAP) of VOCs under low NO_x
73 conditions is significantly higher than that under high NO_x conditions, and the increase
74 of aromatic hydrocarbon emissions caused by coal combustion is the main reason for
75 the higher SOAP in winter (Zhang et al., 2020). Li et al. (2022) found that the average
76 increased concentration of acetylene was 4.8 times from autumn to winter in the
77 Guanzhong Plain, indicating that fuel combustion during the heating period in winter
78 has a significant impact on the composition of VOCs. In contrast, continuous

79 observations conducted by Zhou et al. (2022) in the suburbs of Dongguan in summer
80 found that industrial solvent usage, liquefied petroleum gas (LPG) and oil and gas
81 volatilization were the main sources of VOCs. The results highlighted a wide variation
82 of characteristics, sources and chemical reactions of VOCs in the atmosphere thus it is
83 necessary to investigate VOCs in different cities when formulating control measures.

84 Zhengzhou, as the capital of Henan Province, is an important transportation hub
85 and economic center in the Central Plains region. Zhengzhou is currently facing
86 significant air pollution problems, with the Air Quality Index at the bottom of the
87 national ranking of 168 cities for many years. In January 2023, for example, the number
88 of polluted days with PM_{2.5} as the primary pollutant was 17, and the daily average value
89 of PM_{2.5} reached a maximum of 298 µg/m³
90 ([https://www.aqistudy.cn/historydata/daydata.php?city=%E9%83%91%E5%B7%9E](https://www.aqistudy.cn/historydata/daydata.php?city=%E9%83%91%E5%B7%9E&month=202301)
91 &month=202301, Accessed Jan 2024), which is almost 300% higher than the Chinese
92 daily average standard (grade II, 75 µg/m³). The studies of VOCs were carried out in
93 Zhengzhou in recent years, which focused on the characteristics and sources of VOCs
94 during pollution episodes (Lai et al., 2024) or before the coronavirus epidemic outbreak
95 (Li et al., 2020; Zhang et al., 2021b). While some atmospheric VOCs studies involving
96 the impact of Covid-19 lockdown have been performed in India (Singh et al., 2023a),
97 in China (e.g., Pei et al., 2022; Jensen et al., 2023; Zuo et al., 2024), or with respect to
98 toluene, benzene, m/p-xylene and ethylbenzene only (e.g., Sahu et al., 2022; Singh et
99 al., 2023b), a gap persisted in the investigation of VOCs due to the impact of
100 abolishment of China's zero-policy. Furthermore, some studies have discussed the
101 impact of changes in human production activities on air pollution during and after the
102 outbreak of the coronavirus disease (e.g., Ma et al., 2022; Jiang et al., 2023; Song et al.,
103 2023), but as mentioned earlier, only a few studies with in-depth exploration of the
104 changes in VOCs and none dealing with ending the zero-Covid policy during Omicron
105 variant infection period.

106 In this study, we conducted continuous online observations of VOCs during the
107 polluted winter season at an urban site in Zhengzhou. The study covered the period
108 following the removal of lockdown measures. We focused on pollution events when the
109 daily average PM_{2.5} concentration exceeded 75 µg/m³ (China's Class II standard) for
110 more than three consecutive days. Days with PM_{2.5} concentrations below 35 µg/m³
111 (China's Class I standard) were classified as clean days. During this period, China lifted
112 zero-COVID strategies, announcing the '10 measures' for optimizing COVID-19 rules

113 on December 7, 2022 (http://www.news.cn/politics/2022-12/07/c_1129189285.htm,
114 Accessed Jan 2024). Zhengzhou's epidemic prevention and control measures changed
115 with the issuance of Circular No. 163 on December 4, 2022, which allowed the
116 reopening of closed public places. As a result, movement within Zhengzhou increased
117 and social production resumed. Our research specifically examines the period
118 dominated by the COVID-19 Omicron variant. where they demonstrate notable
119 differences from the early virus strains (i.e., original SARS-CoV-2 virus and Delta) in
120 terms of geographical transmission, the scale of the infected population, and symptom
121 manifestation (Petersen et al., 2022; Merino et al., 2023).

122 After the quarantine policy was lifted, people basically rested at home due to
123 infection or fear of infection with Omicron. The resumption of normal production and
124 life depends on herd immunization. This outbreak event is the longest in duration and
125 the largest in number of infections since the 2020 outbreak of the novel coronavirus in
126 Zhengzhou. It would be beneficial to investigate the impact of this event on emissions
127 related to transportation and industrial production. This change is worth exploring in
128 terms of its impact on transportation and industrial production emissions. Therefore,
129 the characteristics and variations of VOCs during different periods were investigated to
130 assess their impact on the formation of SOA and to provide data support for future
131 pollution control policies in Zhengzhou.

132

133 **2. Materials and methods**

134 **2.1 Sample collection and Chemical analysis**

135 The online VOCs observation station is located on the roof of the Zhengzhou
136 Environmental Protection Monitoring Center, which is in the urban area. The sampling
137 site is close to main roads on three sides (150 m away from Funiu Road on the east side,
138 200 m away from Qinling Road on the west side, and connected to Zhongyuan Road
139 on the south side), and surrounded by residential areas and commercial areas without
140 other large nearby stationary sources. The sampling period for this study was from
141 December 1, 2022, to January 31, 2023, and serious PM_{2.5} pollution in Zhengzhou was
142 of frequent occurrence during December and January.
143 ([https://www.aqistudy.cn/historydata/monthdata.php?city=%e9%83%91%e5%b7%9e](https://www.aqistudy.cn/historydata/monthdata.php?city=%e9%83%91%e5%b7%9e#:~:text=%E7%94%9F%E5%91%BD%E6%9D%A5%E6%BA%90%E8%87%AA%E7%84%B6%EF%BC%8C%E5%81%A5)
144 [#:~:text=%E7%94%9F%E5%91%BD%E6%9D%A5%E6%BA%90%E8%87%AA%](https://www.aqistudy.cn/historydata/monthdata.php?city=%e9%83%91%e5%b7%9e#:~:text=%E7%94%9F%E5%91%BD%E6%9D%A5%E6%BA%90%E8%87%AA%E7%84%B6%EF%BC%8C%E5%81%A5)
145 [E7%84%B6%EF%BC%8C%E5%81%A5](https://www.aqistudy.cn/historydata/monthdata.php?city=%e9%83%91%e5%b7%9e#:~:text=%E7%94%9F%E5%91%BD%E6%9D%A5%E6%BA%90%E8%87%AA%E7%84%B6%EF%BC%8C%E5%81%A5)). Apart from a brief occurrence of rain and
146 snow on December 25, the sampling days were either sunny or cloudy. The wind speed
147 (WS), temperature (Temp) and relative humidity (RH) during this period were 1.3 ± 0.9
148 m/s, 5.3 ± 3.2 °C and $38.9 \pm 19.0\%$), respectively, similar to the values observed in
149 previous years in Zhengzhou. It is interesting to point out that the sampling period in
150 the present study covered the entire infection period of Omicron in Zhengzhou,
151 including the phase of surge in infected population (Infection period, from 2022.12.01
152 to 2022.12.31) and restoration of production and livelihood phase (Recovery period,
153 from 2023.1.1 to 2023.1.31 in 2023) (Fig. S1, Chinese Center for Disease Control and
154 Prevention, 2023).

155 The VOCs were measured hourly using a GC-FID/MS (TH-PKU 300 b, Wuhan
156 Tianhong Instruments Co., China). The instrument TH-PKU300b includes electronic
157 refrigeration ultra-low temperature pre-concentration sampling system, analysis system
158 and system control software. The ambient VOCs in the first 5 minutes of each hour
159 were collected by the sampling system and then entered the concentration system.
160 Under low temperature conditions, the VOCs samples collected were frozen in the
161 capillary capture column, and then quickly heated and resolved, so that the compounds
162 entered the analysis system. After separation by chromatographic column, the
163 compounds were monitored by FID and MS detectors. During the detection process,
164 the atmospheric samples collected undergo analysis through two distinct pathways. C2-
165 C5 hydrocarbons are analyzed using FID, while C5-C12 hydrocarbons, halocarbons,

166 and OVOCs are analyzed with a MS detector. After excluding species with missing data
167 exceeding 10%, the detected volatile organic compounds include 29 alkanes, 11 alkenes,
168 17 aromatics, 35 halocarbons, 12 OVOCs, 1 alkyne (acetylene), and 1 sulfide (CS₂)
169 with a total of 106 compounds. A detailed description of the instrumentation can be
170 found in our previous study (Zhang et al., 2021b; Shi et al., 2022; Zhang et al., 2024).

171 The instrument was calibrated per week to ensure the accuracy of VOCs by
172 injecting standard gases with a five-point calibration curve. The detection limit of C2-
173 C5 hydrocarbons ranges from 0.007 to 0.099 ppbv, other hydrocarbons are 0.004–0.045
174 ppbv, halogenated hydrocarbons 0.009-0.099 ppbv, OVOCs and other compounds of
175 0.006–0.095 ppbv. Thirty-two of the monitored VOCs had over 90% observed data
176 greater than the detection limit, and 34 had more than 50% observed data greater than
177 the detection limit.

178 Simultaneous observations at the same site were also carried out for particulate
179 matter (PM_{2.5}, PM₁₀), other trace gases (carbon monoxide (CO), O₃, nitric oxide (NO),
180 nitrogen dioxide (NO₂)), and meteorological data (Temperature, RH, WS, and wind
181 direction (WD)) based on 1 h resolution.

182 **2.2 Positive Matrix Factorization (PMF) model**

183 EPA PMF5.0 model was used for the quantitative source analysis of VOCs (Norris
184 et al., 2014). The principles and methods have been described in detail in previous
185 studies (Mozaffar et al., 2020; Zhang et al., 2021b). The decomposition of the PMF
186 mass balance equations is simplified as follows (Norris et al., 2014):

187

$$188 \quad x_{ij} = \sum_{k=1}^p g_{ik} f_{kj} + e_{ij} \quad (1)$$

189

190 where x_{ij} is the mass concentration of species j measured in sample i ; g_{ik} is the
191 contribution of factor k to the sample i ; f_{kj} represents the content of the j th species in
192 factor k ; e_{ij} is the residual of species j in sample i ; p represents the number of factors.

193 The fitting objective of the PMF model is to minimize the function Q to obtain the
194 factor contributions and contours. The formula for Q is given in Eq. (2):

195

196
$$Q = \sum_{i=1}^n \sum_{j=1}^m \left[\frac{x_{ij} - \sum_{k=1}^p g_{ik} f_{kj}}{u_{ij}} \right]^2 \quad (2)$$

197

198 where n and m denote the number of samples and VOC species, respectively.

199 Concentrations and uncertainty data are required for the PMF model. In this study,
 200 the median concentration of a given species is used to replace missing values with an
 201 uncertainty of four times of the median values; data less than the Method Detection
 202 Limit (MDL) were replaced with half the MDL, with an uncertainty of 5/6 of the MDL;
 203 and the uncertainty for values greater than the MDL was calculated using Eq. (3). In
 204 Eq. (3), EF is error fraction, expressed as the precision of VOCs species, and the setting
 205 range can be adjusted from 5 to 20% according to the concentration difference (Buzcu
 206 et al., 2006; Song et al., 2007); and c_{ij} is the concentration of species j in sample i :

207
$$U_{ij} = \sqrt{(EF \times c_{ij})^2 + (0.5 \times MDL)^2} \quad (3)$$

208 when the concentration of VOCs in the species is less than the value of the
 209 detection limit U_{ij} is calculated using Eq. (4):

210
$$U_{ij} = \left(\frac{5}{6}\right) MDL \quad (4)$$

211 VOC species and concentration input into PMF were carefully selected to ensure
 212 the accuracy of the PMF results. Species were excluded when over 25% of the samples
 213 were missing or concentrations values were below the MDL (Gao et al., 2018); VOCs
 214 with a short lifetime in the atmosphere were also excluded unless they are source-
 215 relative species (Zhang et al., 2014; Shao et al., 2016). After that, retained VOC species
 216 were categorized according to the signal-to-noise ratio (S/N) with $S/N < 0.2$ species
 217 categorized as bad, $0.2 < S/N < 2$ species categorized as weak; and $S/N > 2$ species
 218 categorized as strong (Shao et al., 2016).

219 We used displacement of factor elements (DISP) to assess PMF modelling
 220 uncertainty (for a description, see Paatero et al. (2014)). Q was less than 1% and no
 221 swaps occurred for the small est dQ^{\max} in DISP. F_{peak} values from -2 to 2 were tested
 222 to explore the rotational stability of the solutions. $Q_{\text{true}}/Q_{\text{exp}}$ is lowest when $F_{\text{peak}} = 0$,
 223 so we chose the PMF results for that case (Fig. S2a). After examining 3-8 factors, 20
 224 base runs with 5 factors eventually selected to represent final result. We provide an
 225 explanation of factor selection in the supplementary materials. Fig. S2(b) includes
 226 $Q_{\text{true}}/Q_{\text{exp}}$, $Q_{\text{robust}}/Q_{\text{exp}}$ for factors 3-8. The slopes of these two ratios in changed at five

227 factors, and we found that five factors were more realistic after repeated comparisons
228 of the results at four, five and six factors.

229 **2.3 SOA generation potential**

230 The contributions of VOC species to SOAP were calculated based on the toluene
231 weighted mass contributions (TMC) method (Derwent et al., 2010). The methodology
232 for calculating SOAP is as follows:

$$234 \text{SOAPF}_i = \frac{\text{VOCs component } i \text{ to SOA mass concentration increments}}{\text{Toluene to SOA mass concentration increment}} \times 100 \quad (5)$$

235

236 SOAPF_i for each VOC is taken from the literature (Derwent et al., 2010). The
237 SOAP was estimated by multiplying the SOAPF_i value by the concentration of
238 individual VOC species. The SOAP calculations through each VOC are as follows:

239

$$240 \text{SOAP} = \sum E_i \times \text{SOAPF}_i \quad (6)$$

241 E_i is the concentration of species i .

242

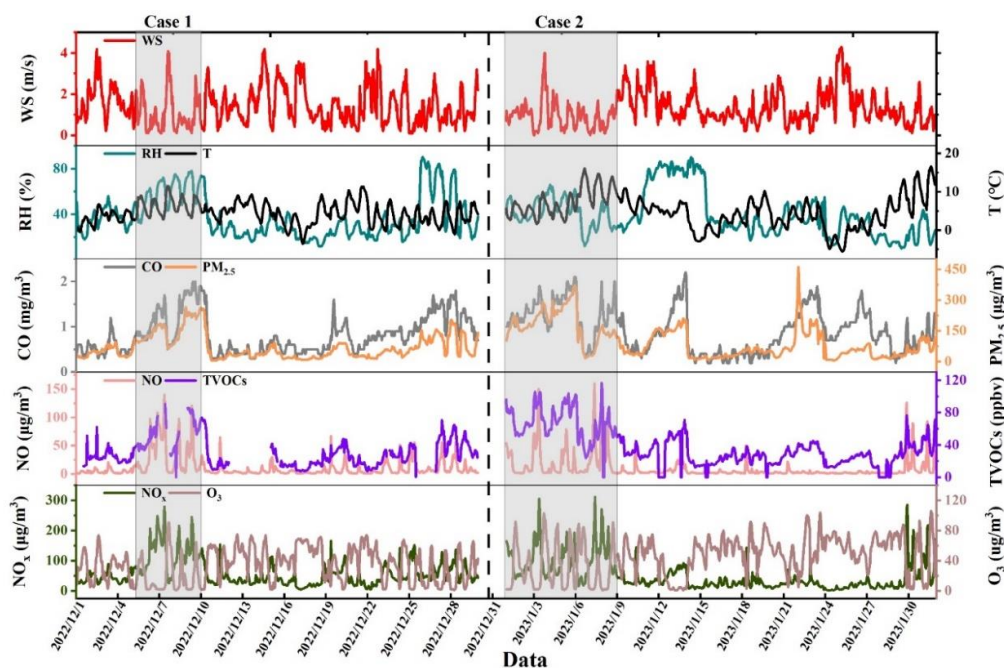
243 **3. Results and discussion**

244 **3.1 Overview of variation in pollutants and meteorological** 245 **parameters**

246 Figure 1 shows the time series of meteorological parameters, TVOCs, O_3 , NO_x ,
247 SO_2 , CO and $\text{PM}_{2.5}$ during the observed periods. Low WS and Temperature were found
248 with an average value of 1.3 ± 0.6 m/s and 5.0 ± 2.5 °C, respectively, during the entire
249 period, comparable with observations at the same site in 2021 (Lai et al., 2024). A total
250 of 62 days of valid data was acquired with the daily average concentration of $\text{PM}_{2.5}$
251 ranging from 53 to 239 $\mu\text{g}/\text{m}^3$, with the average value of 111 ± 45 $\mu\text{g}/\text{m}^3$. The
252 concentration of TVOCs ranged from 15.6 to 57.1 ppbv with an average of 36.1 ± 21.0
253 ppbv, higher than the same period in last year (27.9 ± 12.7 ppbv, Lai et al., 2024).
254 During the observation period, the average values of T, WS and RH were 5.0 ± 2.5 °C,
255 1.3 ± 0.6 m/s and $38.9 \pm 16.7\%$, respectively.

256 Previous studies have shown that meteorological factors such as low WS, high RH,

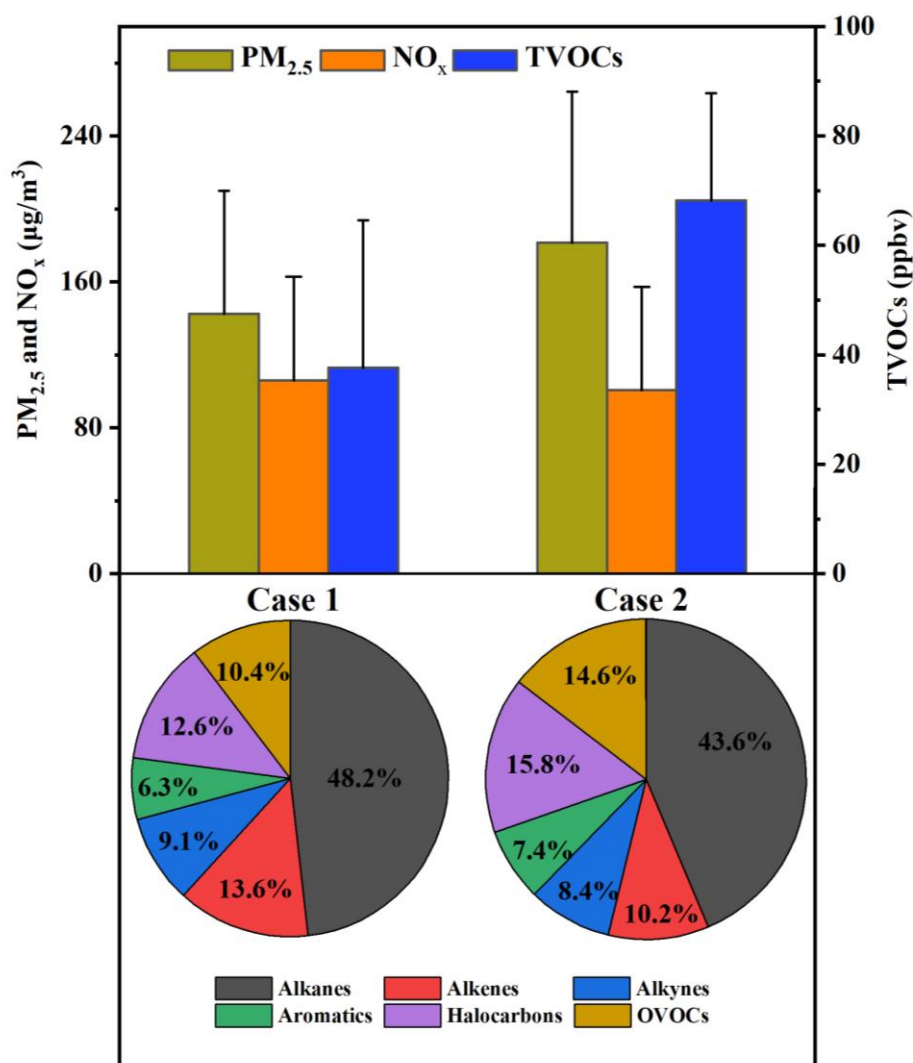
257 and low precipitation are responsible for the increase in PM_{2.5} pollution in Zhengzhou
258 in winter (Duan et al., 2019). Our analysis of the correlation between different
259 pollutants and meteorological conditions during the pollution period showed that
260 PM_{2.5}, TVOCs and NO_x were positively correlated with RH (Fig. S3), which is
261 consistent with the results of some previous studies (Wang et al., 2019). The
262 comparisons of average concentrations of different periods between different periods
263 are presented in Tables 1 and 2. In this study, the WS on clean days (1.4 ± 0.8 m/s)
264 was higher than in Case 1 (1.2 ± 0.9 m/s) and Case 2 (0.9 ± 0.7 m/s), while the RH
265 was lower by 26.2% and 12.5% compared to Case 1 and Case 2, respectively. These
266 findings indicate that high RH and low WS influencing the occurrence of pollution
267 during the observation period, which should be further studied in further. WS, Temp
268 and RH conditions during infection and recovery periods were generally similar, and
269 meteorology may also have played a role in the differences between pollution events,
270 but its specific influence was not determined here. The average concentration of PM_{2.5}
271 during the recovery period was 1.6 times the value during the infection period.
272 Furthermore, the concentrations of other pollutants including SO₂, NO₂, CO, and O₃
273 all showed a similar trend between infection and recovery periods. The TVOC
274 concentration during the recovery period was 1.2 times the value during the infection
275 period, showing an obvious increase trend after resuming production. Decreased
276 trends of air pollutants were found in other studies before and after the outbreak of the
277 novel coronavirus (COVID-19) in early 2020 (Qi et al., 2021; Wang et al., 2021).
278



279

280 Fig. 1. Time series of WS, T, RH, CO, PM_{2.5}, NO, TVOCs, NO_x and O₃ during the observation
 281 period.

282 The shadow section in Fig. 1 represents two haze pollution events during the
 283 monitoring period. A pollution event is determined when the daily average
 284 concentration of PM_{2.5} exceeds 75 µg/m³ (China's II-level standard) for at least three
 285 consecutive days. Case 1 (December 5 to December 10 with daily average PM_{2.5} =
 286 142.5 µg/m³) and Case 2 (January 1 to January 8 with daily average PM_{2.5} = 181.5
 287 µg/m³) were selected as they represent the pollution events in infection and recovery
 288 periods, respectively, due to their long duration and high pollution levels. Any day with
 289 a PM_{2.5} concentration lower than 35 µg/m³ (China's I-level standard) is considered as
 290 Clean day.



291
 292 Fig. 2. The concentration of PM_{2.5}, NO_x, TVOCs and the composition ratio of VOCs in Case 1 and
 293 Case 2.

294 As for the two representative pollution processes (Case 1 during the infection
 295 period and Case 2 during the recovery period), the concentration of TVOCs in Case 1
 296 and Case 2 were 48.4 ± 20.4 and 67.6 ± 19.6 ppbv (Fig. 2), respectively, increased by
 297 63% and 188% compared with values during clean days. The average concentrations
 298 of PM_{2.5} and TVOCs during Case 2 were 1.3 and 1.8 times the values in Case 1. The
 299 highest volume contributions of alkanes were found both in Case 1 (48%) and Case 2
 300 (44%), consistent with the results in the Yangtze River Delta region (36-43%, Liu et al.,
 301 2023). While alkenes exhibited higher volume percentages of 13% in Case 1, followed
 302 by halogenated hydrocarbon (12%) and OVOCs (10%). Higher volume percentages of
 303 alkanes and alkenes in Case 1 were similar to the results in the gasoline evaporation
 304 site in winter (Niu et al., 2022). Equivalent volume contribution of halogenated
 305 hydrocarbon and OVOCs (15%) were found in Case 2, followed by alkenes (10%).

306 Although aromatic hydrocarbons have the lowest volumetric contribution (6% in Case
 307 1 and 7% in Case 2), they show the largest increase from clean days to pollution.

308 Table 1 The average concentrations of meteorological parameters and pollutants during different
 309 processes.

Category	Entire process (2022.12.1- 2023.1.31)	Infection period (2022.12.1- 2022.12.31)	Recovery period (2023.1.1- 2023.1.31)	Case 1 (2022.12.5- 2022.12.10)	Case 2 (2023.1.1- 2023.1.8)	Clean Days
	N = 62 days	N = 31 days	N = 31 days	N = 6 days	N = 8 days	N = 8 days
WS (m/s)	1.3 ± 0.6	1.4 ± 0.6	1.3 ± 0.6	1.2 ± 0.9	0.9 ± 0.7	1.4 ± 0.8
T (°C)	5.0 ± 2.5	4.7 ± 1.7	5.4 ± 3.1	6.1 ± 2.2	7.4 ± 3.5	4.1 ± 3.0
RH (%)	38.9 ± 16.7	37.6 ± 15.5	40.2 ± 18.2	55.7 ± 14.7	42.0 ± 12.1	29.5 ± 18.1
TVOCs (ppbv)	36.1 ± 21.0	31.9 ± 18.1	39.8 ± 22.4	37.6 ± 27.0	68.2 ± 19.6	22.7 ± 11.1
SO ₂ (µg/m ³)	11.4 ± 2.7	10.2 ± 2.8	12.7 ± 2.3	11.0 ± 3.7	16.2 ± 6.1	6.5 ± 2.5
NO ₂ (µg/m ³)	47.2 ± 10.0	46.8 ± 8.6	47.8 ± 11.7	62.7 ± 20.5	65.0 ± 21.3	20.8 ± 15.9
CO (mg/m ³)	0.9 ± 0.2	0.8 ± 0.2	1.1 ± 0.2	1.2 ± 0.5	1.3 ± 0.4	0.5 ± 0.2
O ₃ (µg/m ³)	34.9 ± 6.0	31.1 ± 4.5	39.0 ± 4.6	21.8 ± 23.7	32.5 ± 29.6	52.6 ± 18.4
PM _{2.5} (µg/m ³)	111.5 ± 45.1	86.6 ± 34.6	138.3 ± 39.6	142.5 ± 67.4	181.5 ± 82.7	23.8 ± 16.8

310 Table 2 Concentration of VOC species during different processes (ppbv).

Category	Entire process	Infection period	Recovery period	Case 1	Case 2	Clean days
TVOCs	36.1 ± 21.0	31.9 ± 18.1	39.8 ± 22.4	48.4 ± 20.4	67.6 ± 19.6	17.5 ± 9.5
alkanes	16.8 ± 9.2	15.0 ± 8.4	18.4 ± 9.5	23.1 ± 10.0	29.5 ± 8.4	9.2 ± 5.6
alkenes	4.1 ± 2.7	3.8 ± 2.6	4.4 ± 2.7	6.5 ± 2.9	7.0 ± 2.6	1.7 ± 1.3
alkynes	3.1 ± 2.0	2.7 ± 1.7	3.4 ± 2.1	4.3 ± 2.0	5.8 ± 1.9	1.3 ± 0.8
aromatics	2.1 ± 2.0	1.8 ± 1.5	2.3 ± 2.2	3.0 ± 1.8	4.9 ± 2.8	0.7 ± 0.5
halogenated hydrocarbon	5.4 ± 3.3	4.4 ± 2.3	6.2 ± 3.8	6.0 ± 1.9	10.7 ± 3.6	2.7 ± 1.4
OVOCs	4.6 ± 3.2	3.5 ± 2.7	5.1 ± 3.5	5.0 ± 2.4	9.7 ± 2.8	1.9 ± 1.1

311 3.2 Source Analysis of VOCs

312 Specific VOC ratios can be used for initial source identification of VOCs and
 313 determination of photochemical ages of air masses (Monod et al., 2001; An et al., 2014;
 314 Li et al., 2019). In this study, the ratios of toluene/benzene (T/B), isopentane/n-pentane,
 315 isobutane/n-butane, and m/p-xylene/ethylbenzene (X/E) were selected to initially
 316 identify the potential sources of VOCs (Fig. 3). Concentrations of selected pollutants
 317 and ratios used are shown in Table S1.

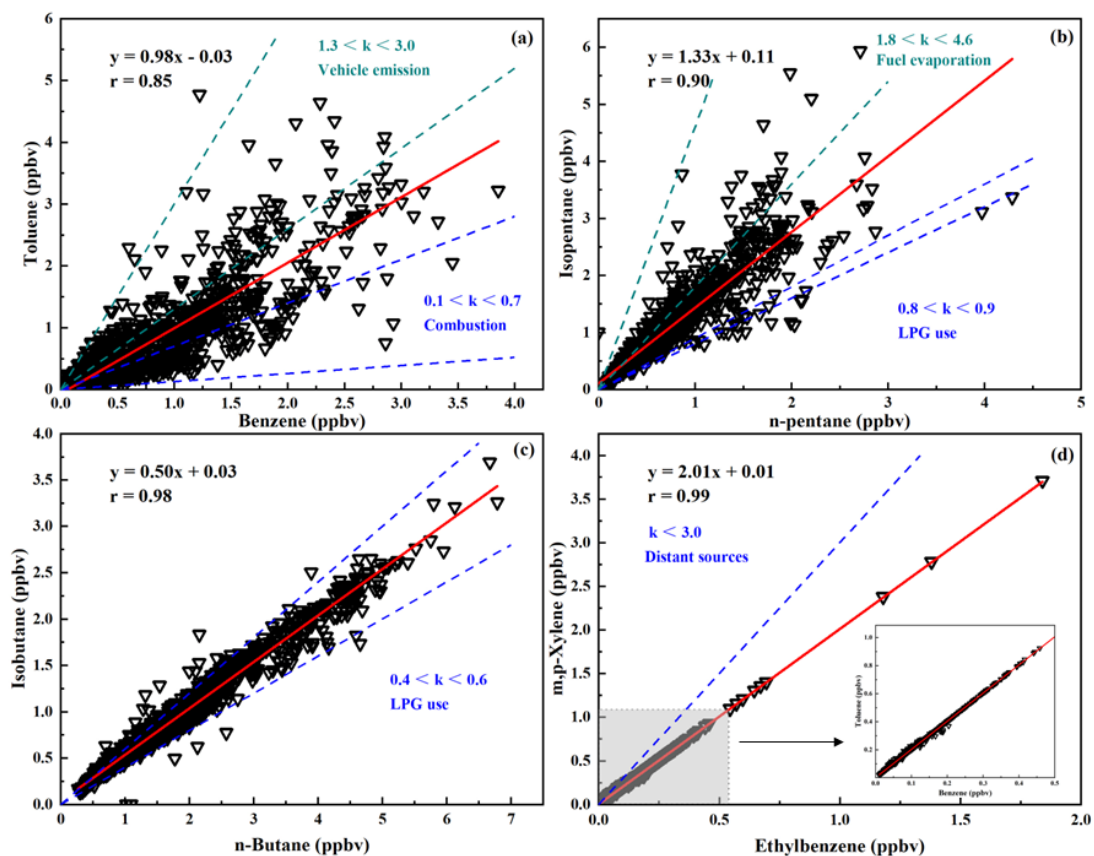
318 The toluene-to-benzene ratio (T/B ratio) was widely used to assess the relative
319 importance of different sources. Specifically, T/B ratio with a value of 1.3-3.0 was
320 observed in vehicle emissions for vehicles with different fuel types (Schauer et al., 2002;
321 Wang et al., 2015). The reported T/B ratio for combustion processes was between 0.13
322 and 0.7 (Li et al., 2011; Wang et al., 2014). The mean value of T/B ratio for the entire
323 period was 1.0, with the majority of the data (99%) falling between 0.1 and 3.0 and
324 concentrated within the 0.7-1.3 range (49%). This suggests that both traffic emissions
325 and combustion may be significant sources of VOCs. It should be noted that this
326 analytical approach is not without limitations. The ratios observed here do not exclude
327 linear combinations from other sources. Consequently, an in-depth examination of the
328 sources of VOCs was conducted using the PMF model in the next section.

329 The isopentane/n-pentane concentration ratios of 0.6-0.8 represent mainly coal
330 combustion emissions, ratios of 0.8-0.9 represent LPG emissions, 2.2-3.8 represent
331 vehicle exhaust emissions, and 1.8-4.6 represent fuel evaporation (Conner et al., 1995;
332 Liu et al., 2008; Li et al., 2019). The sources of isopentane and n-pentane in this study
333 were intricate and multifaceted. The mean isopentane/n-pentane ratio was 1.4, with the
334 majority of data points (99%) falling within the range of 0.1-4.6, with a notable
335 concentration in the 0.8 to 1.8 interval. This indicates that pentane is susceptible to a
336 combination of LPG emissions and fuel evaporation. However, the proportion of
337 pentane may also be affected by a combination of coal combustion emissions and
338 vehicle exhaust.

339 Isobutane/n-butane concentration ratios of 0.2-0.3 represent vehicle emissions,
340 0.4-0.6 represent LPG usage, and 0.6-1.0 represent natural gas emissions (Russo et al.,
341 2010; Zheng et al., 2018). The mean isobutane/n-butane ratio in this study was 0.5, with
342 the majority of data points (99%) falling within the 0.4-0.6 range, indicating that VOCs
343 at the observation sites were significantly influenced by the use of LPG. (Shao et al.,
344 2016; Zeng et al., 2023). This result can also be caused by a combination of vehicle
345 exhaust and natural gas emissions.

346 The ratio of X/E can be used to infer the photochemical age of the air mass. X/E
347 ratios around 2.5-2.9 are typical of urban areas, indicating that VOCs are mainly from
348 the urban area (fresh air mass) (Kumar et al., 2018). When this ratio is significantly
349 lower than 3.0, it indicates that VOCs are mainly transported from distant sources
350 (aging air masses) (Kumar et al., 2018). The average X/E value in this study was 2.0
351 (Fig. 3(d)), indicating low photochemical activity and aging of the air mass at the

352 observation site. Potential source analyses also indicate that air masses are affected by
353 long-range transport (Fig. S4).



354

355 Fig. 3. Correlation analysis between specific VOC species.

356 Figure 4 shows the chemical profiles of individual VOCs resolved by the PMF
357 model during the entire observation period. These five factors eventually selected as
358 potential sources for the observed VOCs are: (1) Fuel evaporation; (2) Solvent usage;
359 (3) Vehicular emission; (4) Industrial source; and (5) Combustion. These 5 factors have
360 been commonly reported before, e.g., in Shijiazhuang, northern China (Guan et al, 2023)
361 and in Beijing (Cui et al., 2022).

362 Alkanes of C4-C6 substances were predominant in factor 1, including 2-
363 methylpentane, 3-methylpentane, isobutane, n-butane, isopentane and n-pentane from
364 oil and gas (Xiong et al., 2020). Fig. S5 shows that emissions from this source peak at
365 midday, when fuel volatilization is high, The CPF plot shows that south-east is the
366 dominant direction at WS of less than 2 m/s (Fig. 5a). Therefore, factor 1 was identified
367 as the source of oil and gas volatilization.

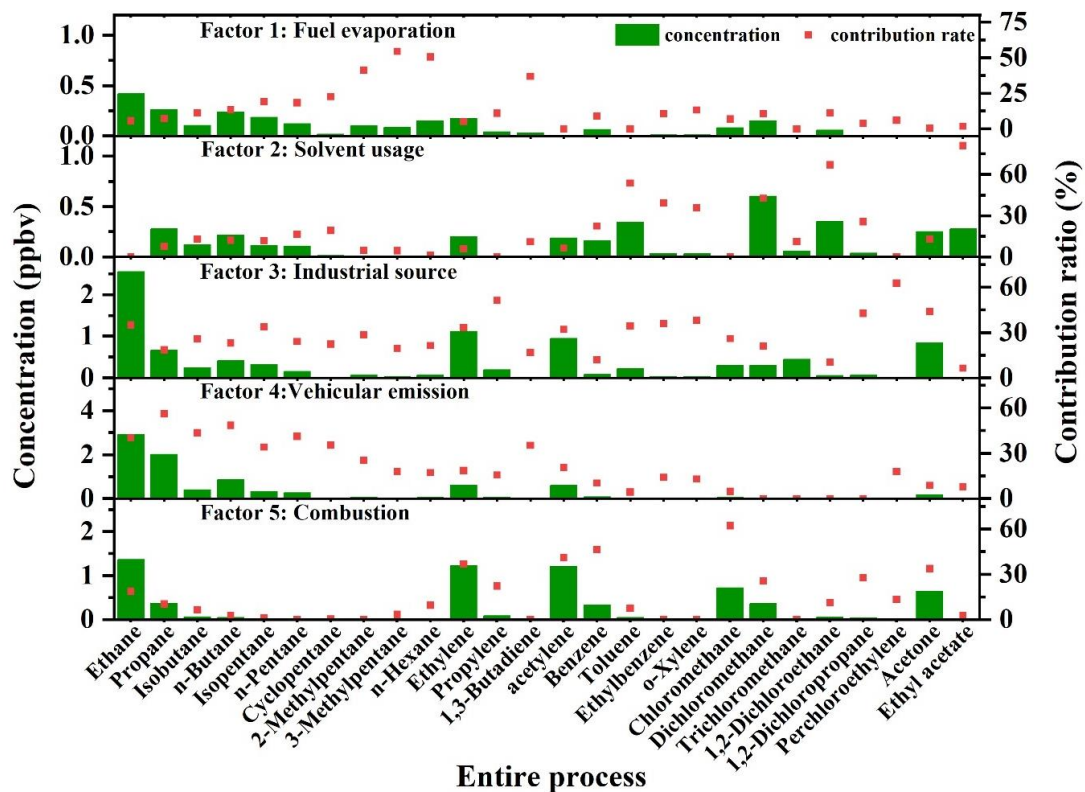
368 The contribution of benzene, toluene, methylene chloride, 1,2-dichloroethane and

369 ethyl acetate was high in factor 2. It has been shown that benzene, toluene, ethylbenzene,
370 and xylene is an important component in the use of solvents (Li et al., 2015); methylene
371 chloride is often used as a chemical solvent, while esters are mostly used as industrial
372 solvents or adhesives (Li et al., 2015). Factor 2 is determined to be solvent usage source.
373 The CPF plot shows that due east is the main emission direction at WS less than 2 m/s
374 and southeast is the main source at WS greater than 2 m/s (Fig. 5b).

375 Factor 3 contains predominantly C3-C8 alkanes, olefins and alkynes, and
376 relatively high concentrations of benzene. These substances are usually emitted by
377 industrial processes (Shao et al., 2016), so Factor 4 is defined as an industrial source.
378 The CPF plots indicate that a local source at low WS is the dominant sources (Fig. 5c).

379 Factor 4 is characterized by relatively high levels of C2-C6 low-carbon alkanes
380 (ethane, propane, isopentane, n-pentane, isobutane and n-butane), olefins (ethylene and
381 propylene), and benzene and toluene, which are important automotive exhaust tracers
382 (Song et al., 2021; Zhang et al., 2021b). Ethylene and propylene are important
383 components derived from vehicle-related activities. Previous studies of VOCs in
384 Zhengzhou have shown a high percentage of VOCs emitted from gasoline vehicles,
385 with the main source of alkanes being on-road mobile sources (Bai et al., 2020). The
386 daily variation of this source in Fig. S5 shows a bimodal trend, with peaks occurring in
387 the morning and evening peaks of traffic, consistent with motor vehicle emissions. Fig.
388 5d shows that this source is mainly from the west where WS is below 2 m/s, and in this
389 direction, there are a number of urban arterial roads with high traffic volumes.
390 Therefore, factor 4 was defined as vehicular emission source.

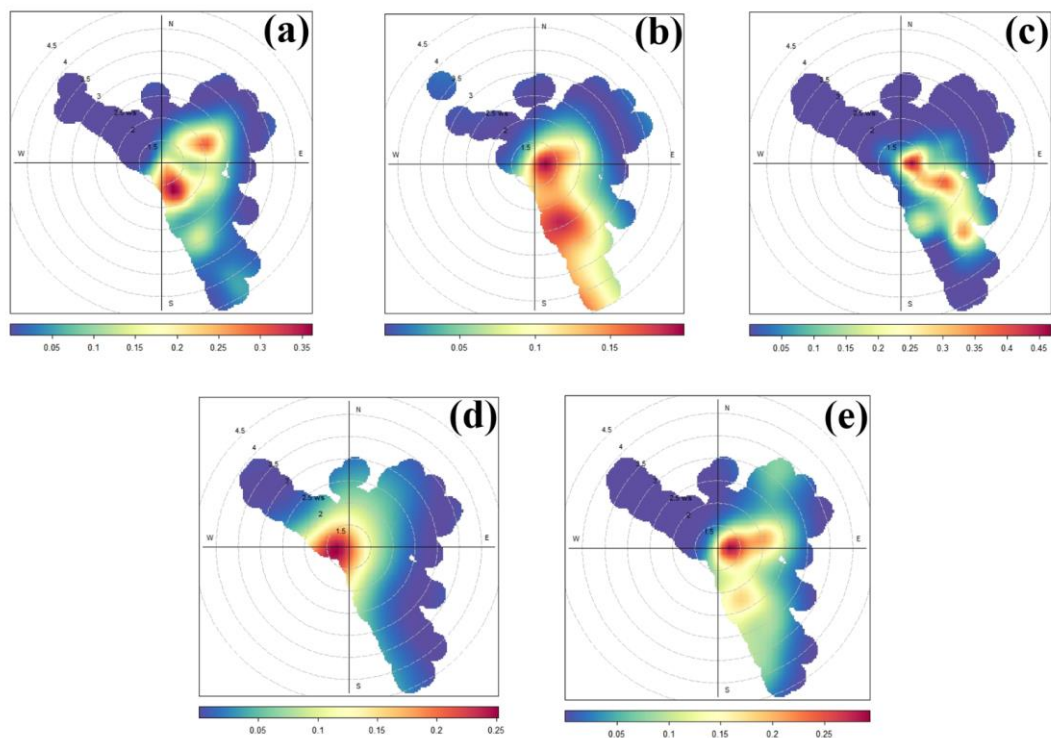
391 The highest contribution to factor 5 is chloromethane (62%). Benzene (46%) and
392 acetylene (41%) also contribute highly to factor 5. Chloromethane is the key tracer for
393 biomass combustion and acetylene is the key tracer for coal combustion (Xiong et al.,
394 2020). Therefore, factor 5 is defined as a combustion source. The CPF plot shows that
395 at WS below 2 m/s, the north-east direction is the dominant source direction (Fig. 5e).



396

397

Fig. 4. Concentration of VOC species in each factor and contribution to each source.



398

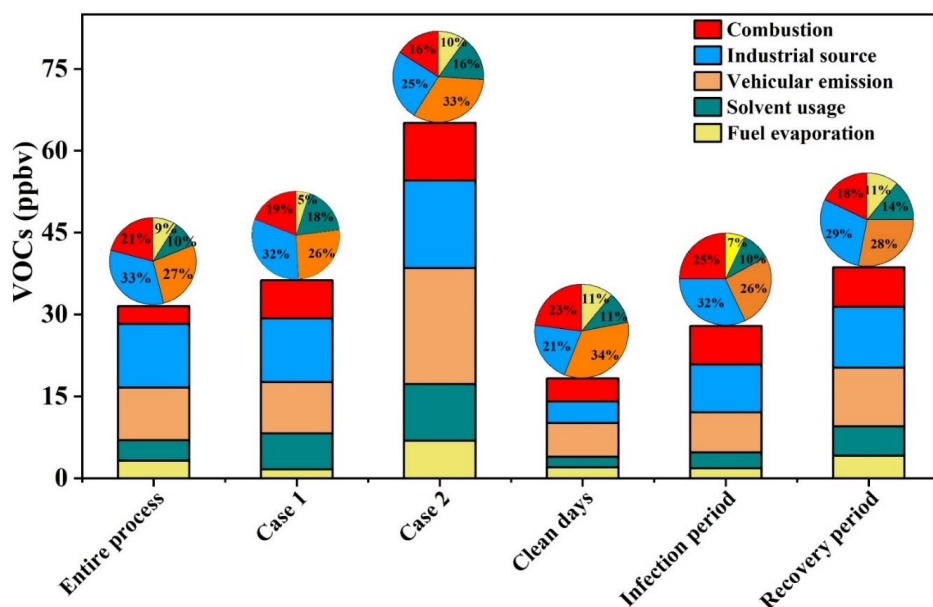
399

Fig. 5. CPF plots of five VOCs sources obtained using the PMF model.

400 Note: a: Fuel evaporation; b: Solvent usage; c: Industrial source; d: Vehicular emission; e:
 401 Combustion.

402 Fig. S6 compares the differences in PMF source profiles between the Omicron
 403 infection period and the recovery period, as well as between the pollution day and the
 404 clean day. We present the concentrations of the five main VOCs in all five factors in
 405 Table S2. Ethane (vehicular emission), 2-methylpentane (fuel evaporation), benzene
 406 (industry source), chloromethane (combustion), and ethyl acetate (solvent usage) were
 407 selected as tracers for five sources. Ethane concentration in Case 2 (5.9 ppbv) is much
 408 higher than in other processes, and ethane concentration during the recovery period (3.4
 409 ppbv) is also higher than during the infection period (2.4 ppbv), which may to some
 410 extent reflect increased vehicular emissions during the recovery period.

411 Concentrations of most species were significantly higher during the recovery
 412 period than during the infection period. The representative pollution processes in both
 413 periods showed the same results as well, with a 79% higher concentration of TVOCs in
 414 Case 2 (65.1 ppbv) compared to Case 1 (36.3 ppbv) (Fig. 6). While in Case 1 industry
 415 was the dominant source of VOCs, by Case 2 motorized sources reached a
 416 concentration value of 21.2 ppbv, accounting for 33% of the observed VOCs, and
 417 became the dominant source of emissions. This is consistent with the fact that people's
 418 mobility activities have increased after the epidemic has entered the recovery period.
 419 As a group of VOCs species with the highest concentration share, ethane and propane
 420 contributed more to the clean days motor vehicle source than other processes, which
 421 also resulted in a 34% clean days motor vehicle source share.



422

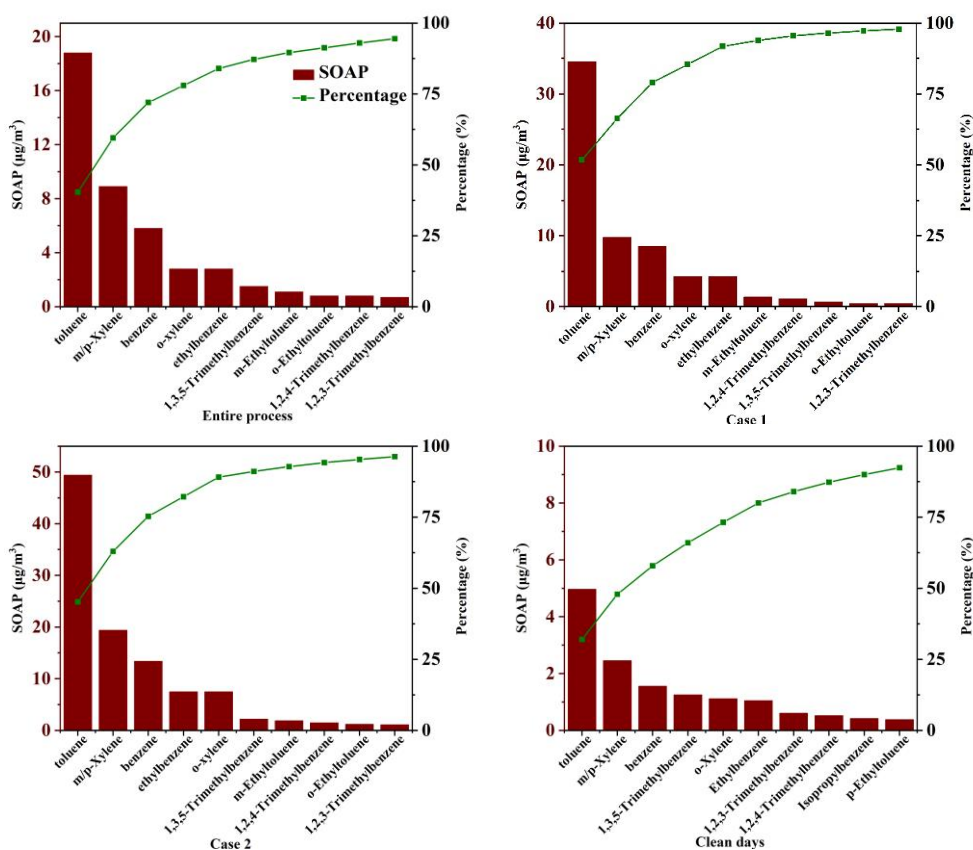
423

Fig. 6. Contribution of each to VOCs for different processes.

424 **3.3 SOAP**

425 VOCs are estimated to contribute about 16–30% or more of PM_{2.5} by mass through
 426 SOA production (Huang et al., 2014). Therefore, by calculating the SOAP value, the
 427 influence of different sources on PM_{2.5} production can be reflected to a certain extent.

428 We have included quantitative analysis for SOAP as well. Fig. 7 shows the SOAP
 429 concentrations and contribution rates of the top ten species throughout the entire
 430 process, during two pollution processes, and clean days. The top ten species all reached
 431 close to 100% of the total SOAP contribution, with Case 1 reaching 98%. In each
 432 process, the composition of the top ten substances is essentially the same. Aromatic
 433 hydrocarbons contributed the most, with BTEX always occupying the top five positions
 434 and toluene the most. The SOAP values of the top ten contributing species for the two
 435 polluting processes are shown in Tables S3 and S4. Toluene, the highest contributing
 436 species, reached a SOAP value of 49.4 $\mu\text{g}/\text{m}^3$ in the most polluted Case 2, which was
 437 3.2 times higher than the SOAP sum of all species on the clean day (15.5 $\mu\text{g}/\text{m}^3$). The
 438 SOAP value for Case 1, which is also a contaminated process, was 67 $\mu\text{g}/\text{m}^3$, and the
 439 main species (m/xylene: 9.8 $\mu\text{g}/\text{m}^3$, benzene: 8.5 $\mu\text{g}/\text{m}^3$) including toluene (34.6 $\mu\text{g}/\text{m}^3$)
 440 were lower than those for Case 2 (m/xylene: 19.4 $\mu\text{g}/\text{m}^3$, benzene: 13.4 $\mu\text{g}/\text{m}^3$).



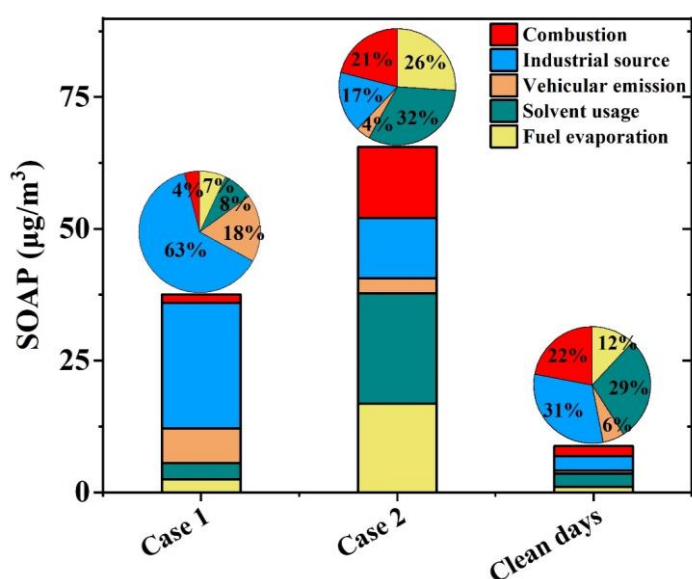
441

442

Fig. 7. SOAP dominant species in different processes

443

444 Figure 8 shows the SOAP calculated after source resolution of the two pollution
445 processes by PMF for clean days, respectively. In Case 1, industrial source is the
446 dominant source with a contribution ratio of 63%. In Case 2, the pollution sources
447 exhibit a more evenly distributed contribution, where the solvent usage and fuel
448 evaporation sources emerge as the primary contributors to SOAP, with their respective
449 contribution levels rising to 32% and 26%. Case 1 was during the infection period,
450 when social activities had not yet returned to normal. In Case 2, when society had
451 basically returned to normal, the increase in emissions from various sources resulted in
452 a more balanced distribution of SOAP contributions and caused more severe PM_{2.5}
453 pollution. In addition, a few days before Case 2, the Zhengzhou Municipal People's
454 Government initiated the Heavy Pollution Weather Level II response (<https://sthjj.zhengzhou.gov.cn/tzgg/7037130.jhtml>) and introduced control measures
455 for emissions from industrial and mobile sources, which resulted in a significant
456 reduction of SOAP levels from industrial and motorized sources in Case 2. The clean
457 day result with a SOAP of 8.8 $\mu\text{g}/\text{m}^3$ also indicates that industrial and solvent usage
458 sources are the most dominant SOAP sources. The primary sources of aromatic
459 compounds, which are the most significant contributors to SOAP, are solvent usage and
460 industrial process emissions. This finding aligns with the results of other studies (Wu
461 et al., 2017). Consequently, it is imperative to implement measures to reduce PM_{2.5}
462 pollution by regulating emissions from industrial and solvent usage sources.



463

464

Fig. 8. SOAP value and contribution ratio of each process

465

466 4. Conclusions

467 Continuous observation of VOCs during the infection of the Omicron epidemic
468 was carried out at an urban site in polluted Zhengzhou from December 1, 2022, to
469 January 31, 2023. The daily average concentration of PM_{2.5} ranged from 53.5 to 239.4
470 μg/m³ with an average value of 111.5 ± 45.1 μg/m³ during the whole period. The
471 concentration of TVOCs ranged from 15.6 to 57.1 ppbv with an average of 36.1 ± 21.0
472 ppbv, higher than the same period in last year (27.9 ± 12.7 ppbv, Lai et al., 2024). Two
473 representative contamination processes were identified (Case 1 during the infection
474 period and Case 2 during the recovery period). While the meteorological conditions of
475 the two pollution processes are relatively similar, the specific impacts caused thereby
476 have yet to be determined. The concentration of TVOCs in Case 1 and Case 2 were 48.4
477 ± 20.4 and 67.6 ± 19.6 ppbv, respectively, increased by 63% and 188% compared with
478 values during clean days. The average concentrations of PM_{2.5} and TVOCs during Case
479 2 were 1.3 and 1.8 times of the values in Case 1. This is consistent with the observed
480 increase in pollutant emissions following the return to normal social life from the period
481 of Omicron infection. The highest volume contributions of alkanes were found both in
482 Case 1 (48%) and Case 2 (44%). Though the volume contribution of aromatics were
483 the lowest (6% in Case 1 and 7% in Case 2), the highest increase ratio was found from
484 clean days to polluted episodes. Low WS and high RH were the main meteorological
485 reasons for the occurrence of pollution. Analyzing the sources of VOCs revealed that
486 VOCs were found to be affected by a combination of local emissions and regional
487 transport. The primary sources of atmospheric VOCs in Zhengzhou were identified as
488 industrial emissions (32%), vehicle emissions (27%), and combustion (21%).
489 Significant discrepancies were observed in the sources of VOCs between the two
490 pollution processes. In Case 1, industrial emissions constituted the primary source of
491 VOCs, accounting for 32% of the total VOC concentration. In contrast, in Case 2, the
492 proportion of vehicle emissions increased to 33%, representing the primary source of
493 VOCs.

494 A further analysis of the effect of VOCs on SOA generation reveals that aromatic
495 compounds are the primary contributors to SOAP, with BTEX being the predominant
496 contributor throughout the period. The SOAP values reached 37.6 and 65.6 μg/m³ in
497 Case 1 and Case 2, respectively. In Case 1, the greatest contribution to SOAP was made
498 by industrial sources (63%, 23.8 μg/m³), while vehicular sources, which constituted the

499 second most important source, accounted for only 18%. In Case 2, the contribution of
500 each VOC source was more evenly distributed, with solvent use sources and fuel
501 evaporation sources representing the primary contributors to SOAP, accounting for 32%
502 (20.9 $\mu\text{g}/\text{m}^3$) and 26% (16.8 $\mu\text{g}/\text{m}^3$), respectively. The SOAP result for the clean day
503 was 8.8 $\mu\text{g}/\text{m}^3$, with industrial sources and solvent use still being the primary
504 contributors. Therefore, the industrial and solvent use sectors are the predominant
505 sources of pollutants during this observation. The aforementioned results substantiate
506 the considerable impact of elevated emissions from all sources on the exacerbation of
507 pollution following the conclusion of the Omicron infection.

508 **Author contribution:**

509 Bowen Zhang: Data curation, Methodology, Formal analysis, Writing Original Draft.

510 Dong Zhang: Data curation, Formal analysis, Review & Editing.

511 Zhe Dong: Data curation, Formal analysis, Review & Editing.

512 Xinshuai Song: Data curation, Formal analysis.

513 Ruiqin Zhang: Supervision, Writing-Review & Editing, Funding acquisition.

514 Xiao Li: Formal analysis, Investigation, Supervision, Writing-Review & Editing.

515 **Competing interests:**

516 The contact author has declared that none of the authors has any competing interests.

517 **Acknowledgments:**

518 This research was supported by the Natural Science Foundation of Henan Province
519 (232300421395) and the National Key Research and Development Program of China
520 (2017YFC0212400).

521 **References**

522 An, J., Zhu, B., Wang, H., Li, Y., Lin, X., and Yang, H.: Characteristics and source
523 apportionment of VOCs measured in an industrial area of Nanjing, Yangtze River Delta,
524 China, *Atmospheric Environment*, 97, 206-214,
525 <https://doi.org/10.1016/j.atmosenv.2014.08.021>, 2014.

526 Bai, L., Lu, X., Yin, S., Zhang, H., Ma, S., Wang, C., Li, Y., and Zhang, R.: A
527 recent emission inventory of multiple air pollutant, $\text{PM}_{2.5}$ chemical species and its
528 spatial-temporal characteristics in central China, *Journal of Cleaner Production*, 269,

529 122114, <https://doi.org/10.1016/j.jclepro.2020.122114>, 2020.

530 Buzcu, B. and Fraser, M. P.: Source identification and apportionment of volatile
531 organic compounds in Houston, TX, *Atmospheric Environment*, 40, 2385-2400,
532 <https://doi.org/10.1016/j.atmosenv.2005.12.020>, 2006.

533 Conner, T. L., Lonneman, W. A., Seila, R.L.: Transportation-related volatile
534 hydrocarbon source profiles measured in atlanta, *Journal of the Air & Waste*
535 *Management Association*, 45 (5), 383-394,
536 <https://doi.org/10.1080/10473289.1995.10467370>, 1995.

537 Cui, L., Wu, D., Wang, S., Xu, Q., Hu, R., and Hao, J.: Measurement report:
538 Ambient volatile organic compound (VOC) pollution in urban Beijing: characteristics,
539 sources, and implications for pollution control, *Atmospheric Chemistry and Physics*,
540 22, 11931-11944, <https://doi.org/10.5194/acp-22-11931-2022>, 2022.

541 Derwent, R. G., Jenkin, M. E., Utembe, S. R., Shallcross, D. E., Murrells, T. P.,
542 and Passant, N. R.: Secondary organic aerosol formation from a large number of
543 reactive man-made organic compounds, *Science of the Total Environment*, 408, 3374-
544 3381, <https://doi.org/10.1016/j.scitotenv.2010.04.013>, 2010.

545 Duan, S., Jiang, N., Yang, L., Zhang, R.: Transport Pathways and Potential Sources
546 of PM_{2.5} During the Winter in Zhengzhou, *Environmental Science*, Jan 8;40(1):86-93,
547 <https://doi.org/10.13227/j.hjkx.201805187>, 2019.

548 Gao, J., Zhang, J., Li, H., Li, L., Xu, L., Zhang, Y., Wang, Z., Wang, X., Zhang,
549 W., Chen, Y., Cheng, X., Zhang, H., Peng, L., Chai, F., and Wei, Y.: Comparative study
550 of volatile organic compounds in ambient air using observed mixing ratios and initial
551 mixing ratios taking chemical loss into account – A case study in a typical urban area
552 in Beijing, *Science of the Total Environment*, 628-629, 791-804,
553 <https://doi.org/10.1016/j.scitotenv.2018.01.175>, 2018.

554 Guan, Y., Liu, X., Zheng, Z., Dai, Y., Du, G., Han, J., Hou, L. a., and Duan, E.:
555 Summer O₃ pollution cycle characteristics and VOCs sources in a central city of
556 Beijing-Tianjin-Hebei area, China, *Environmental Pollution*, 323, 121293,
557 <https://doi.org/10.1016/j.envpol.2023.121293>, 2023.

558 Huang, R., Zhang, Y., Bozzetti, C. et al.: High secondary aerosol contribution to p
559 articulate pollution during haze events in China, *Nature*, 514 (7521), 218–22, <https://doi.org/10.1038/nature13774>, 2014.

561 Hui, L., Liu, X., Tan, Q., Feng, M., An, J., Qu, Y., Zhang, Y., Deng, Y., Zhai, R., a
562 nd Wang, Z.: VOC characteristics, chemical reactivity and sources in urban Wuhan, ce

563 ntral China, Atmospheric Environment, 224, 117340, <https://doi.org/10.1016/j.atmose>
564 [nv.2020.117340](https://doi.org/10.1016/j.atmose), 2020.

565 Jensen, A., Liu, Z., Tan, W., Dix, B., Chen, T., Koss, A., Zhu, L., Li, L., de Gouw,
566 J.: Measurements of volatile organic compounds during the COVID-19 lockdown in
567 Changzhou, China, Geophysical research letters, 48(20), <https://doi.org/10.1029/2021>
568 [GL095560](https://doi.org/10.1029/2021), 2021.

569 Jiang, N., Hao, X., Hao, Q., Wei, Y., Zhang, Y., Lyu, Z., Zhang, R.: Changes in se
570 condary inorganic ions in PM_{2.5} at different pollution stages before and after COVID-1
571 9 control, Environmental Science, 44(5), 2430-2440, <https://doi.org/10.13227/j.hjkx.2>
572 [02206170](https://doi.org/10.13227/j.hjkx.2), 2023.

573 Kumar, A., Singh, D., Kumar, K., Singh, B. B., and Jain, V. K.: Distribution of
574 VOCs in urban and rural atmospheres of subtropical India: Temporal variation, source
575 attribution, ratios, OFP and risk assessment, Science of the Total Environment, 613-614,
576 492-501, <https://doi.org/10.1016/j.scitotenv.2017.09.096>, 2018.

577 Lai, M., Zhang, D., Yin, S., Song, X., and Zhang, R.: Pollution characteristics,
578 source apportionment and activity analysis of atmospheric VOCs during winter and
579 summer pollution in Zhengzhou City, Environmental Science, 4108, 3500-3510,
580 <https://doi.org/10.13227/j.hjkx.202001133>, 2024.

581 Li, B., Ho, S. S. H., Gong, S., Ni, J., Li, H., Han, L., Yang, Y., Qi, Y., and Zhao,
582 D.: Characterization of VOCs and their related atmospheric processes in a central
583 Chinese city during severe ozone pollution periods, Atmospheric Chemistry and
584 Physics, 19, 617-638, <https://doi.org/10.5194/acp-19-617-2019>, 2019.

585 Li, J., Deng, S., Tohti, A., Li, G., Yi, X., Lu, Z., Liu, J., and Zhang, S.: Spatial
586 characteristics of VOCs and their ozone and secondary organic aerosol formation
587 potentials in autumn and winter in the Guanzhong Plain, China, Environmental
588 Research, 211, 113036, <https://doi.org/10.1016/j.envres.2022.113036>, 2022.

589 Li, J., Xie, S. D., Zeng, L. M., Li, L. Y., Li, Y. Q., and Wu, R. R.: Characterization
590 of ambient volatile organic compounds and their sources in Beijing, before, during, and
591 after Asia-Pacific Economic Cooperation China 2014, Atmospheric Chemistry and
592 Physics, 15, 7945-7959, <https://doi.org/10.5194/acp-15-7945-2015>, 2015.

593 Li, J., Lu, K., Lv, W., Li, J., Zhong, L., Ou, Y., Chen, D., Huang, X., and Zhang,
594 Y.: Fast increasing of surface ozone concentrations in Pearl River Delta characterized
595 by a regional air quality monitoring network during 2006–2011, Journal of
596 Environmental Sciences, 26, 23-36, [https://doi.org/10.1016/S1001-0742\(13\)60377-0](https://doi.org/10.1016/S1001-0742(13)60377-0),

597 2014.

598 Liu, Y., Li, X., Tang, G., Wang, L., Lv, B., Guo, X., and Wang, Y.: Secondary
599 organic aerosols in Jinan, an urban site in North China: Significant anthropogenic
600 contributions to heavy pollution, *Journal of Environmental Sciences*, 80, 107-115,
601 <https://doi.org/10.1016/j.jes.2018.11.009>, 2019.

602 Liu, Y., Shao, M., Fu, L., Lu, S., Zeng, L., and Tang, D.: Source profiles of volatile
603 organic compounds (VOCs) measured in China: Part I, *Atmospheric Environment*, 42,
604 6247-6260, <https://doi.org/10.1016/j.atmosenv.2008.01.070>, 2008.

605 Liu, Y., Song, M., Liu, X., Zhang, Y., Hui, L., Kong, L., Zhang, Y., Zhang, C., Qu,
606 Y., An, J., Ma, D., Tan, Q., and Feng, M.: Characterization and sources of volatile
607 organic compounds (VOCs) and their related changes during ozone pollution days in
608 2016 in Beijing, China, *Environmental Pollution*, 257, 113599,
609 <https://doi.org/10.1016/j.envpol.2019.113599>, 2020.

610 Liu, Z., Hu, K., Zhang, K., Zhu, S., Wang, M., and Li, L.: VOCs sources and roles
611 in O₃ formation in the central Yangtze River Delta region of China, *Atmospheric
612 Environment*, 302, <https://doi.org/10.1016/j.atmosenv.2023.119755>, 2023.

613 Li, X., Wang, S., Hao, J.: Characteristics of volatile organic compounds (VOCs)
614 emitted from biofuel combustion in China, *Environmental Science*, 32, 3515-3521,
615 2011.

616 Li, Y., Yin, S., Zhang R., Yu, S., Yang, J., and Zhang, D.: Characteristics and source
617 apportionment of atmospheric VOCs at different pollution levels in winter in an urban
618 area in Zhengzhou, *Environmental Science*, 4108, 3500-3510,
619 <https://doi.org/10.13227/j.hjkx.202001133>, 2020.

620 Ma, Q., Wang, W., Wu, Y., Wang, F., Jin, L., Song, Y., Han, Y., Zhang, R., Zhang,
621 D.: Haze caused by NO_x oxidation under restricted residential and industrial activities
622 in a mega city in the south of North China Plain, *Chemosphere*, Volume 305, 135489,
623 <https://doi.org/10.1016/j.chemosphere.2022.135489>, 2022.

624 Merino, M., Marinescu, M., Cascajo, A., Carretero, J., Singh, D.: Evaluating the
625 spread of Omicron COVID-19 variant in Spain, *Future Generation Computer Systems*,
626 149, 547-561, <https://doi.org/10.1016/j.future.2023.07.025>, 2023.

627 Monod, A., Sive, B. C., Avino, P., Chen, T., Blake, D. R., and Sherwood Rowland,
628 F.: Monoaromatic compounds in ambient air of various cities: a focus on correlations
629 between the xylenes and ethylbenzene, *Atmospheric Environment*, 35, 135-149,
630 [https://doi.org/10.1016/S1352-2310\(00\)00274-0](https://doi.org/10.1016/S1352-2310(00)00274-0), 2001.

631 Mozaffar, A., Zhang, Y.-L., Fan, M., Cao, F., and Lin, Y.-C.: Characteristics of
632 summertime ambient VOCs and their contributions to O₃ and SOA formation in a
633 suburban area of Nanjing, China, *Atmospheric Research*, 240, 104923,
634 <https://doi.org/10.1016/j.atmosres.2020.104923>, 2020.

635 Mu, L., Feng, C., Li, Y., Li, X., Liu, T., Jiang, X., Liu, Z., Bai, H., and Liu, X.:
636 Emission factors and source profiles of VOCs emitted from coke production in Shanxi,
637 China, *Environmental Pollution*, 335, 122373,
638 <https://doi.org/10.1016/j.envpol.2023.122373>, 2023.

639 Niu, Y., Yan, Y., Chai, J., Zhang, X., Xu, Y., Duan, X., Wu, J., and Peng, L.: Effects
640 of regional transport from different potential pollution areas on volatile organic
641 compounds (VOCs) in Northern Beijing during non-heating and heating periods,
642 *Science of the Total Environment*, 836, 155465,
643 <https://doi.org/10.1016/j.scitotenv.2022.155465>, 2022.

644 Norris, G., Duvall, R., Brown, S., Bai, S. EPA Positive Matrix Factorization (PMF)
645 5.0 Fundamentals and User Guide. U.S. Environmental Protection Agency, Washington,
646 DC, EPA/600/R-14/108 (NTIS PB2015-105147), 2014.

647 Paatero, P., Eberly, S., Brown, S. G., Norris, G. A.: Methods for estimating
648 uncertainty in factor analytic solutions, *Atmospheric Measurement Techniques*, Volume
649 7, 781-797, <https://doi.org/10.5194/amt-7-781-2014>, 2014.

650 Pei, C., Yang, W., Zhang, Y., Song, W., Xiao, S., Wang, J., Zhang, J., Zhang, T.,
651 Chen, D., Wang, Y., Chen, Y., Wang, X.: Decrease in ambient volatile organic
652 compounds during the COVID-19 lockdown period in the Pearl River Delta region,
653 south China, *Science of The Total Environment*, 823, 153720,
654 <https://doi.org/10.1016/j.scitotenv.2022.153720>, 2022.

655 Petersen, M. S., Í Kongsstovu, S., Eliasen, E. H., Larsen, S., Hansen, J. L., Vest,
656 N., Dahl, M. M., Christiansen, D. H., Møller, L. F., & Kristiansen, M. F.: Clinical
657 characteristics of the Omicron variant - results from a Nationwide Symptoms Survey
658 in the Faroe Islands, *International Journal of Infectious Diseases*, 122, 636–643,
659 <https://doi.org/10.1016/j.ijid.2022.07.005>, 2022.

660 Qi, J., Mo, Z., Yuan, B., Huang, S., Huangfu, Y., Wang, Z., Li, X., Yang, S., Wang,
661 W., Zhao, Y., Wang, X., Wang, W., Liu, K., and Shao, M.: An observation approach in
662 evaluation of ozone production to precursor changes during the COVID-19 lockdown,
663 *Atmospheric Environment*, 262, 118618,
664 <https://doi.org/10.1016/j.atmosenv.2021.118618>, 2021.

665 Russo, R. S., Zhou, Y., White, M. L., Mao, H., Talbot, R., and Sive, B. C.: Multi-
666 year (2004–2008) record of nonmethane hydrocarbons and halocarbons in New
667 England: seasonal variations and regional sources, *Atmospheric Chemistry and Physics*,
668 10, 4909-4929, <https://doi.org/10.5194/acp-10-4909-2010>, 2010.

669 Sahu, L. K., Tripathi, N., Gupta, M., Singh, V., Yadav, R., Patel, K.: Impact of
670 COVID-19 Pandemic lockdown in ambient concentrations of aromatic volatile organic
671 compounds in a metropolitan city of western India, *Journal of geophysical research*,
672 *Atmospheres : JGR*, 127(6), <https://doi.org/10.1029/2022JD036628>, 2022.

673 Schauer, J., Kleeman, M., Cass, G., Simoneit, B.: Measurement of emissions from
674 air pollution sources.5. C₁-C₃₂ organic compounds from gasoline-powered motor
675 vehicles, *Environmental Science & Technology*, 36, 1169-1180,
676 <https://doi.org/10.1021/es0108077>, 2002.

677 Shao, P., An, J., Xin, J., Wu, F., Wang, J., Ji, D., and Wang, Y.: Source
678 apportionment of VOCs and the contribution to photochemical ozone formation during
679 summer in the typical industrial area in the Yangtze River Delta, China, *Atmospheric
680 Research*, 176-177, 64-74, <https://doi.org/10.1016/j.atmosres.2016.02.015>, 2016.

681 Shi, Y., Liu, C., Zhang, B., Simayi, M., Xi, Z., Ren, J., and Xie, S.: Accurate
682 identification of key VOCs sources contributing to O₃ formation along the Liaodong
683 Bay based on emission inventories and ambient observations, *Science of the Total
684 Environment*, 844, 156998, [10.1016/j.scitotenv.2022.156998](https://doi.org/10.1016/j.scitotenv.2022.156998), 2022.

685 Singh, B., Sohrab, S., Athar, M., Alandijany, T., Kumari, S., Nair, A., Kumari, S.,
686 Mehra, K., Chowdhary, K., Rahman, S., Azhar, E.: Substantial changes in selected
687 volatile organic compounds (VOCs) and associations with health risk assessments in
688 industrial areas during the COVID-19 Pandemic, *Toxics*, 11, 165,
689 <https://doi.org/10.3390/toxics11020165>, 2023a.

690 Singh, B., Singh, M., Ulman, Y., Sharma, U., Pradhan, R., Sahoo, J., Padhi, S.,
691 Chandra, P., Koul, M., Tripathi, P., Kumar, D., Masih, J.: Distribution and temporal
692 variation of total volatile organic compounds concentrations associated with health risk
693 in Punjab, India, *Case Studies in Chemical and Environmental Engineering*, 8, 100417,
694 <https://doi.org/10.1016/j.cscee.2023.100417>, 2023b.

695 Song, M., Li, X., Yang, S., Yu, X., Zhou, S., Yang, Y., Chen, S., Dong, H., Liao,
696 K., Chen, Q., Lu, K., Zhang, N., Cao, J., Zeng, L., and Zhang, Y.: Spatiotemporal
697 variation, sources, and secondary transformation potential of volatile organic
698 compounds in Xi'an, China, *Atmospheric Chemistry and Physics*, 21, 4939-4958,

699 <https://doi.org/10.5194/acp-21-4939-2021>, 2021.

700 Song, X., Zhang, D., Li, X., Lu, X., Wang, M., Zhang, B., Zhang, R.: Simultaneous
701 observations of peroxyacetyl nitrate and ozone in Central China during static
702 management of COVID-19: Regional transport and thermal decomposition,
703 *Atmospheric Research*, Volume 294, 106958,
704 <https://doi.org/10.1016/j.atmosres.2023.106958>, 2023.

705 Song, Y., Shao, M., Liu, Y., Lu, S., Kuster, W., Goldan, P., and Xie, S.: Source
706 apportionment of ambient volatile organic compounds in Beijing, *Environmental*
707 *Science & Technology*, 41, 4348-4353, <https://doi.org/10.1021/es0625982>, 2007.

708 Wang, H., Li, J., Peng, Y., Zhang, M., Che, H., Zhang, X.: The impacts of the
709 meteorology features on PM_{2.5} levels during a severe haze episode in central-east China,
710 *Atmospheric Environment*, Volume 197, Pages 177-189, ISSN 1352-2310,
711 <https://doi.org/10.1016/j.atmosenv.2018.10.001>, 2019.

712 Wang, H., Wang, Q., Chen, J. Chen, C., Huang, C., Qiao, L. Lou, S., Lu, J.: Do
713 vehicular emissions dominate the source of C6–C8 aromatics in the megacity Shanghai
714 of eastern China?, *Environmental Science*, 27, 290-297, [https://doi.org/10.](https://doi.org/10.1016/j.jes.2014.05.033)
715 [1016/j.jes.2014.05.033](https://doi.org/10.1016/j.jes.2014.05.033), 2015.

716 Wang, M., Lu, S., Shao, M., Zeng, L., Zheng, J., Xie, F., Lin, H., Hu, K., and Lu,
717 X.: Impact of COVID-19 lockdown on ambient levels and sources of volatile organic
718 compounds (VOCs) in Nanjing, China, *Science of the Total Environment*, 757, 143823,
719 <https://doi.org/10.1016/j.scitotenv.2020.143823>, 2021.

720 Wang, M., Zeng, L., Lu, S., Shao, M., Liu, X., Yu, X., Chen, W., Yuan, B., Zhang,
721 Q., Hu, M., & Zhang, Z.: Development and validation of a cryogen-free automatic gas
722 chromatograph system (GC-MS/FID) for online measurements of volatile organic
723 compounds, *Analytical Methods*, 6, 9424, <https://doi.org/10.1039/C4AY01855A>, 2014.

724 Wang, T., Xue, L., Brimblecombe, P., Lam, Y. F., Li, L., and Zhang, L.: Ozone
725 pollution in China: A review of concentrations, meteorological influences, chemical
726 precursors, and effects, *Science of the Total Environment*, 575, 1582-1596,
727 <https://doi.org/10.1016/j.scitotenv.2016.10.081>, 2017.

728 Wu, R., Li, J., Hao, Y., Li, Y., Zeng, L., and Xie, S.: Evolution process and sources
729 of ambient volatile organic compounds during a severe haze event in Beijing, China,
730 *Science of the Total Environment*, 560-561, 62-72,
731 <https://doi.org/10.1016/j.scitotenv.2016.04.030>, 2016.

732 Wu, W., Zhao, B., Wang, S., and Hao, J.: Ozone and secondary organic aerosol

733 formation potential from anthropogenic volatile organic compounds emissions in China,
734 Journal of Environmental Sciences, 53, 224-237,
735 <https://doi.org/10.1016/j.jes.2016.03.025>, 2017.

736 Xiong, Y., Zhou, J., Xing, Z., and Du, K.: Optimization of a volatile organic
737 compound control strategy in an oil industry center in Canada by evaluating ozone and
738 secondary organic aerosol formation potential, Environmental Research, 191, 110217,
739 <https://doi.org/10.1016/j.envres.2020.110217>, 2020.

740 Yun, L., Li, C., Zhang, M., He, L. and Guo, J.: Pollution characteristics and sources
741 of atmospheric VOCs in the coastal background area of the Pearl River Delta,
742 Environmental Science, 4191-4201, <https://doi.org/10.13227/j.hjkk.202101155>, 2021.

743 Zeng, X., Han, M., Ren, G., Liu, G., Wang, X., Du, K., Zhang, X., and Lin, H.: A
744 comprehensive investigation on source apportionment and multi-directional regional
745 transport of volatile organic compounds and ozone in urban Zhengzhou, Chemosphere,
746 334, 139001, <https://doi.org/10.1016/j.chemosphere.2023.139001>, 2023.

747 Zhang, C., Liu, X., Zhang, Y., Tan, Q., Feng, M., Qu, Y., An, J., Deng, Y., Zhai, R.,
748 Wang, Z., Cheng, N., and Zha, S.: Characteristics, source apportionment and chemical
749 conversions of VOCs based on a comprehensive summer observation experiment in
750 Beijing, Atmospheric Pollution Research, 12, 230-241,
751 <https://doi.org/10.1016/j.apr.2020.12.010>, 2021a.

752 Zhang, D., He, B., Yuan, M., Yu, S., Yin, S., and Zhang, R.: Characteristics,
753 sources and health risks assessment of VOCs in Zhengzhou, China during haze
754 pollution season, Journal of Environmental Sciences, 108, 44-57,
755 <https://doi.org/10.1016/j.jes.2021.01.035>, 2021b.

756 Zhang, D., Li, X., Yuan, M., Xu, Y., Xu, Q., Su, F., Wang, S., Zhang, R.:
757 Characteristics and sources of nonmethane volatile organic compounds (NMVOCs) and
758 O₃-NO_x-NMVOC relationships in Zhengzhou, China, Atmosphere Chemistry and
759 Physics, 24, 8549-8567, <https://doi.org/10.5194/acp-24-8549-2024>, 2024.

760 Zhang, F., Shang, X., Chen, H., Xie, G., Fu, Y., Wu, D., Sun, W., Liu, P., Zhang,
761 C., Mu, Y., Zeng, L., Wan, M., Wang, Y., Xiao, H., Wang, G., and Chen, J.: Significant
762 impact of coal combustion on VOCs emissions in winter in a North China rural site,
763 Science of the Total Environment, 720, 137617,
764 <https://doi.org/10.1016/j.scitotenv.2020.137617>, 2020.

765 Zhang, J., Sun, Y., Wu, F., Sun, J., and Wang, Y.: The characteristics, seasonal
766 variation and source apportionment of VOCs at Gongga Mountain, China, Atmospheric

767 Environment, 88, 297-305, <https://doi.org/10.1016/j.atmosenv.2013.03.036>, 2014.

768 Zhang, Z., Yan, X., Gao, F., Thai, P., Wang, H., Chen, D., Zhou, L., Gong, D., Li,
769 Q., Morawska, L., and Wang, B.: Emission and health risk assessment of volatile
770 organic compounds in various processes of a petroleum refinery in the Pearl River Delta,
771 China, Environmental Pollution, 238, 452-461,
772 <https://doi.org/10.1016/j.envpol.2018.03.054>, 2018.

773 Zheng, H., Kong, S., Xing, X., Mao, Y., Hu, T., Ding, Y., Li, G., Liu, D., Li, S.,
774 and Qi, S.: Monitoring of volatile organic compounds (VOCs) from an oil and gas
775 station in northwest China for 1 year, Atmospheric Chemistry and Physics, 18, 4567-
776 4595, <https://doi.org/10.5194/acp-18-4567-2018>, 2018.

777 Zheng, J., Zhong, L., Wang, T., Louie, P. K. K., and Li, Z.: Ground-level ozone in
778 the Pearl River Delta region: Analysis of data from a recently established regional air
779 quality monitoring network, Atmospheric Environment, 44, 814-823,
780 <https://doi.org/10.1016/j.atmosenv.2009.11.032>, 2010.

781 Zhou, Z., Xiao, L., Fei, L., Yu, W., Lin M., Huang, T., Zhang, Z. and Tao J.:
782 Characteristics and sources of VOCs during ozone pollution and non-pollution periods
783 in summer in Dongguan industrial concentration area, Environmental Science, 4497-
784 4505, <https://doi.org/10.13227/j.hjkx.202111285>, 2022.

785 Zou, Y., Yan, X. L., Flores, R. M., Zhang, L. Y., Yang, S. P., Fan, L. Y., Deng, T.,
786 Deng, X. J., and Ye, D. Q.: Source apportionment and ozone formation mechanism of
787 VOCs considering photochemical loss in Guangzhou, China, Science of the Total
788 Environment, 903, 166191, <https://doi.org/10.1016/j.scitotenv.2023.166191>, 2023.

789 Zuo, H., Jiang, Y., Yuan, J., Wang, Z., Zhang, P., Guo, C., Wang, Z., Chen, Y., Wen,
790 Q., Wei, Y., Li, X.: Pollution characteristics and source differences of VOCs before and
791 after COVID-19 in Beijing, Science of The Total Environment, 907, 167694,
792 <https://doi.org/10.1016/j.scitotenv.2023.167694>, 2024.

793